Deep Space Network

211
Wideband Very-Long Baseline Interferometry

Document Owner:			Approved By:	
Signature Provided	05/16/2022		Signature Provided	04/29/2022
Lisa Mauger	Date		Timothy Pham	Date
VRA Software CDE			Communications Systems Chief Engineer	
Prepared By:			Released by:	
Signature Provided	05/15/2022		Signature Provided	06/07/2022
Dong Shin	Date		Christine Chang	Date
System Engineer			DSN Document Release Authority	

DSN No. **810-005, 211, Rev. F**
Issue Date: June 07, 2022
JPL D-19379; CL# 22-2651

Jet Propulsion Laboratory
California Institute of Technology

Review Acknowledgment

By signing below, the signatories acknowledge that they have reviewed this document and provided comments, if any, to the signatories on the Cover Page.

Signature Provided	04/19/2022	Signature Provided	03/25/2022
Jeff Berner	Date	Alina Bedrossian	Date
DSN Project Chief Engineer		Science System Engineer	

Signature Provided	04/28/2022
Harvey Soldan	
Group Supervisor, DSN System Engineering	

Document Change Log

Rev	Issue Date	Prepared By	Affected Sections or pages	Change Summary
Initial	8/25/2006	Kurt Liewer	All	All
A	4/15/2011	Kurt Liewer	Section 2, 2.1, 2.3 Figure 2, 2.3.3, 2.3.5, and 2.4	• Removed references to Mark III VLBI DAT • Replaced all instances of "radio telescope" to "antenna" • Added text noting new DAT system will be replacing old in 2013. • Removed EAC references • Noted termination of Mark-IV tape support • Updated Figure 2 to reflect changes in the system
B	02/09/2015	A. Bedrossian J. S. Border D. Shin	Section 2 and Appendix	• Removed DTE, DAT and PCFS • Added DVP and Mark 5C • Added DSS—26, -35, -54 • Updated Figures, Tables, and Appendix
C	02/10/17	J. S. Border D. Shin	Section 2.3	Added DSS-36. Removed DSS-45.
D	07/03/18	D. Shin A. Bedrossian	Section 2 and 3	Remove DSS-15 and update section 2.3
E	12/23/2019	D. Shin A. Bedrossian	Section 2.2, 2.3, Figure 2, 2.3.4, Table 2 and 4	• 2.2: Example of the efficiency gain is updated • 2.3: Capacity of the open-loop receiver is updated. • 2.3.4: Tone generator availability at BWG antennas is updated • Figure 2, Table 2, Table 4: Updated
F	06/07/2022	D. Shin A. Bedrossian	Section 1.2, 2.3, 2.3.1, 2.3.3, 2.3.4, 2.3.5, and 2.4, Figure 1, 2 Table 1, 2, and 3	• 1.2: Added Module 108 (Ka-band source catalog) • 2.3: Updated for VRA/EJVC • 2.3.1: Added DSS-53, DSS-56, and K-band • 2.3.3: Updated for VRA/EJVC • 2.3.4: Updated for VRA/EJVC • 2.3.5: Updated for EJVC • 2.4: Updated for VRA/EJVC and added K-band • Figure 1: Updated for VRA/EJVC • Figure 2: Added DSS-53/56 and K-band and updated for VRA/EJVC • Table 1: Added DSS-53/56 and K-band

Rev	Issue Date	Prepared By	Affected Sections or pages	Change Summary
				• Table 2: Added supported bandwidths • Table 3: Updated and add DSS-53/56

Contents

Figures

Tables

1 Introduction

1.1 Purpose

This module provides an introduction to the Very-Long Baseline Interferometry (VLBI) astrometric measurement technique and identifies the capabilities and performance of Deep Space Network (DSN) equipment used to support wideband VLBI measurements.

1.2 Scope

The content of this module is limited to a discussion of the data gathering and data processing equipment used by the DSN to support VLBI. Experiment design and the quality of the results are influenced by many other factors that are discussed in Section 2.4. Among these factors are antenna performance parameters discussed in modules 101, 103 and 104, and frequency reference performance discussed in module 304. VLBI experimenters may also be interested in station locations discussed in module 301 and extra-galactic radio source positions provided in module 107 and 108. It should be noted that the equipment discussed in this module is the major contributor to the information content of modules 301, 107, and 108.

2 General Information

The DSN uses its VLBI capability to measure the earth orientation parameters that establish the relationship of the Terrestrial Reference Frame containing its stations to the Celestial Reference Frame used for spacecraft navigation. VLBI is also used to determine the relative locations of its stations and the locations of extra-galactic radio sources (EGRSs). The EGRSs are used as reference points for delta-differential one-way ranging (ΔDOR) spacecraft navigation (see module 210). Because the DSN uses equipment that is compatible with that used by the international VLBI community, other agencies can coordinate their observation schedules with DSN scheduled activities and the resultant data can be shared between the DSN and external experimenters.

2.1 Description of Very-Long Baseline Interferometry

Very-Long Baseline Interferometry is a technique for measuring the precise time difference between the arrivals of waveforms originating from an EGRS at two (or more) stations. Figure 1 provides an illustration of the technique. The stations simultaneously observe an EGRS. As they are widely separated, their baseline, B, passes through the Earth. At each station, the instantaneous voltage of the received signal (a random Gaussian process) is recorded in each of several channels; this is known as VLBI data acquisition. The measured difference in arrival time can be converted to an approximate path length difference by multiplying by c, the speed of electromagnetic waves in a vacuum. In actuality, the conversion is much more complex as the wave front must pass through several layers of the Earth's atmosphere – each of which has a different propagation speed.
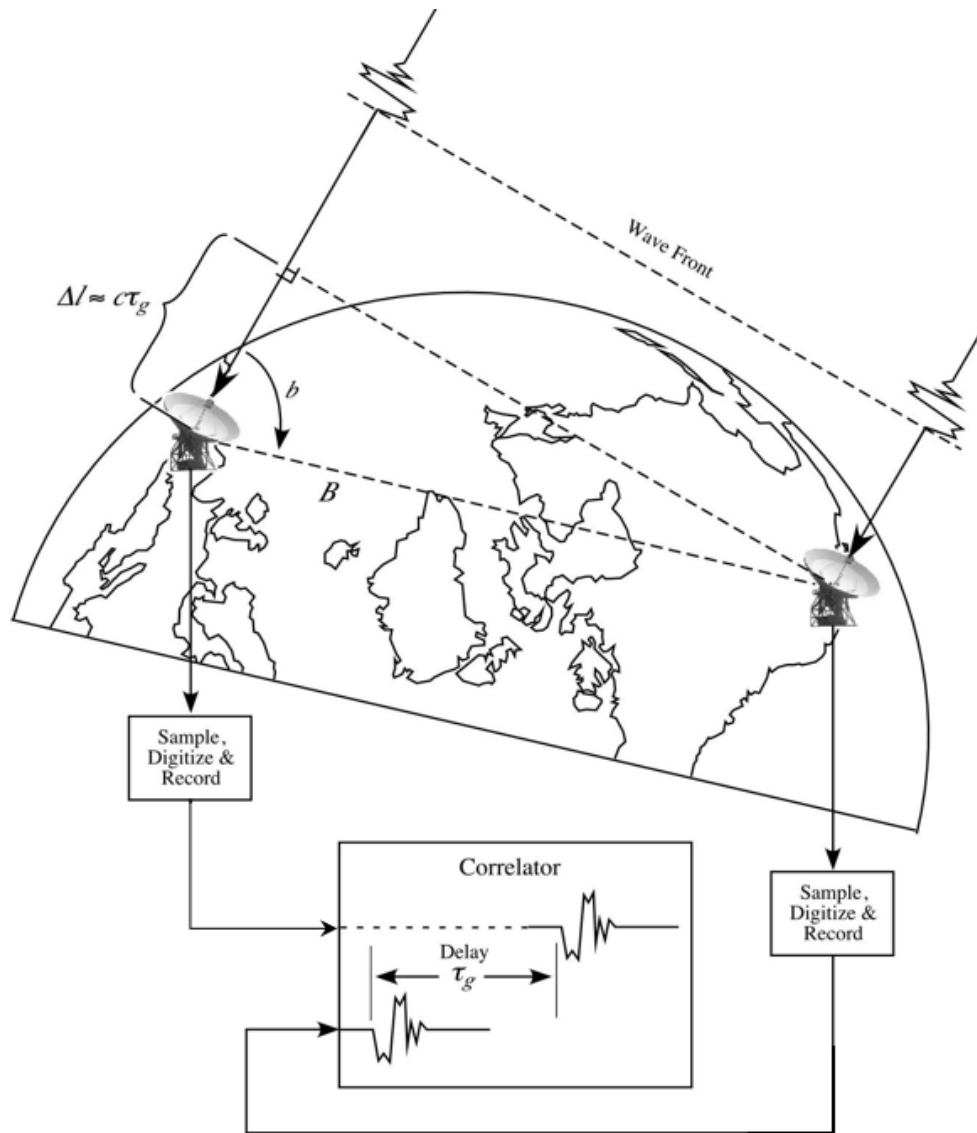
Figure 1. Very-Long Baseline Interferometry

The recorded data from the participating antennas are brought together at a correlator. The data from matching channels at the different radio telescopes are cross-correlated to determine the geometric time delay, τ_g; this is known as VLBI data correlation. After converting the time delay to a path length by a process that takes into account atmospheric delay and other effects, the angular relationship between the baseline of the two stations and the radio source can be determined by the relationship $b = \cos^{-1}(\Delta l / B)$. It is important to note that this is not a complete solution for the angular position in the sky of the radio source. This calculation only provides information about the location of the radio source in the plane defined by the interferometer baseline and the direction of arrival. The correlation of data from the observation of additional radio sources is necessary to completely define the baseline. By making sufficient

observations and assuming some reference, it is possible to calculate a singular solution that estimates each station's coordinates, the angular positions of all observed sources, the offset and rate differences between the two station frequency references, and several parameters relating to propagation. Additional observations above the minimum enable statistical uncertainties in the estimation to be reduced. A complete discussion of the process is contained in Reference 1.

The precision of a VLBI measurement improves with the length of the baseline. The location of the DSN stations provides baselines of 66% (Goldstone to Madrid) and 83% (Goldstone to Canberra) of the Earth's diameter. The third baseline, Canberra to Madrid, is 98% of the Earth's diameter but provides very limited mutual visibility (see module 301). To mitigate mutual visibility effects, additional antennas are often involved in VLBI measurements allowing a station between DSN locations to serve as a "relay" to tie-together observations made in different portions of the sky during an observation session.

2.2 Bandwidth Synthesis

The signal-to-noise ratio obtained by correlating the signals from two observing stations depends on the characteristics of the stations, the bandwidth of the channel being correlated and the observation time. It can be calculated from the following expression.

$$SNR_{CH} = 2.05 \times 10^{-4} (\gamma_v S) D_1 D_2 \sqrt{\frac{\eta_1 \eta_2 B_{CH} T}{T_{Sys1} T_{Sys2}}} \qquad (1)$$

where

$(\gamma_v S)$	= correlated flux density where S is the total flux density (jansky)
D_1, D_2	= antenna diameters (m)
η_1, η_2	= antenna efficiencies
B_{CH}	= channel bandwidth (Hz)
T	= observation time (s)
T_{Sys1}, T_{Sys2}	= antenna system noise temperatures (K)

The factor 2.05 x 10^{-4} includes all normalization constants and allowances for degradation due to one-bit quantization and the fact that only one polarization is received.

When multiple channels are being correlated simultaneously and they have approximately the same SNR_{CH}, the post-correlation SNR for use in equation (3) can be calculated by

$$SNR = \sqrt{n} \cdot SNR_{CH} \qquad (2)$$

where n is the number of channels in the correlation.

The error in delay measurement resulting from the correlation of data from two VLBI stations is expressed by

$$\sigma = \frac{c}{2\pi \cdot SNR \cdot BW} \tag{3}$$

where

c = the speed of electromagnetic propagation

SNR = the post-correlation signal-to-noise ratio

BW = the observation bandwidth

It can be seen from equation (3) that an extremely large data volume for transport to the common correlation site would be needed if the entire bandwidth were recorded. For example, if a post-correlation SNR of 40 (16 dB) is available, a bandwidth of 125 MHz would be required to achieve a delay error of 1 cm.

The data volume is significantly reduced by the technique of *bandwidth synthesis* (Reference 2). This technique uses several narrow channels spread across the observation bandwidth to achieve an *RMS bandwidth* of

$$BW_{RMS} = \sqrt{\frac{\sum_{CH=1}^{n}(f_{CH} - f_{AVG})^2}{n}} \tag{4}$$

where

f_{CH} = center frequency of each channel used in the bandwidth synthesis

f_{AVG} = the average of all channel center frequencies used in the bandwidth synthesis

n = the number of channels

As an example of the efficiency gained by bandwidth synthesis, a typical Ka-band VLBI measurement will use the eleven 32-MHz double-sided channels shown in Table 4 corresponding to an RMS bandwidth of 168.314 MHz. By employing hard limiting, two-bit quantization, and a sampling rate equal to twice the bandwidth of each channel, the total recorded bandwidth is reduced to 128 MHz.

2.3 DSN VLBI Support Equipment

A diagram showing the major items of DSN equipment used to support wideband VLBI is provided by Figure 2. DSN 34-m BWG antennas and 70-m antennas are available for VLBI data acquisition. Note that 70-m antenna is not recommended for VLBI observations due to its slow slew rate.
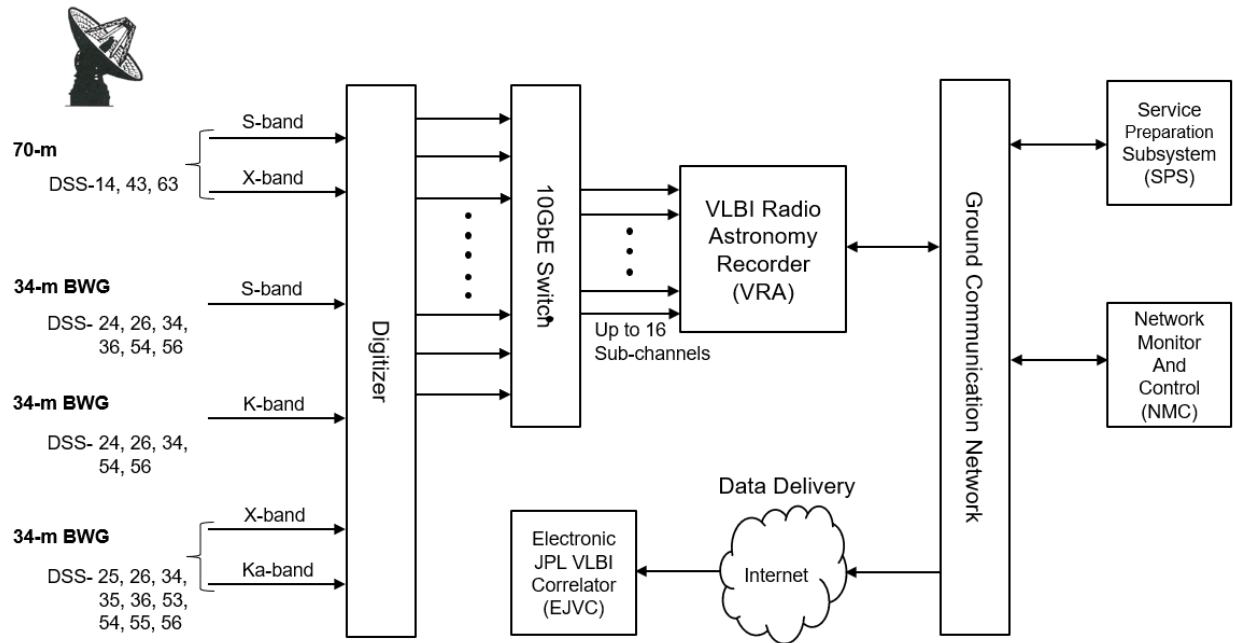
Figure 2. DSN Equipment for Wideband VLBI Support

Received signals are processed by the Deep Space Communication Complex (DSCC) VLBI Radio Astronomy Recorder (VRA). The VLBI data is electronically transmitting to the Electronic JPL VLBI correlator (EJVC) for the correlation. The VRA interfaces directly with the DSN Network Monitor and Control (NMC) Subsystem.

2.3.1   Signal Reception

Signals that are collected by the antenna are amplified by a cryogenically-cooled low-noise amplifier (LNA). For every observation band, the LNA is followed by a downconverter that translates the radio-frequency signal to an intermediate frequency (IF) to be forwarded to the Signal Processing Center (SPC). The downconverters are located on the antenna and are derived from the station frequency standard. Their local oscillator (LO) frequencies are 2.0 GHz for S-band, 8.1 GHz for X-band, variable 25.503 GHz +/- 487.5 MHz for K-band, and 31.7 GHz for Ka-band.

The frequency and polarization capabilities of the DSN for VLBI are summarized in Table 1.

Subnet	DSS	S-band	X-band	K-band	Ka-band
70-m	14, 43, & 63	RCP and LCP (2200–2300 MHz)	RCP and LCP (8200–8600 MHz)	–	–
34-m BWG	24, 26, 34, 36, 54, & 56	RCP or LCP (2200–2300 MHz)	–	–	–
	24, 26, 34, 54, & 56	–	–	RCP or LCP (25.5–27.0 GHz)	–
	34, 54	–	RCP or LCP (8200–8600 MHz)	–	RCP and LCP (31.8–32.3 GHz)
	25, 26, 35, 36, 53, 55, & 56	–	RCP and LCP (8200–8600 MHz)	–	RCP and LCP (31.8–32.3 GHz)

Table 1. Frequency and Polarization Support Capabilities for VLBI

2.3.2 *Subreflector Position*

Gravity deformation of the primary reflector and the structure that supports the subreflector as the antenna moves in elevation causes a change in the antenna focal position. To compensate for this, the subreflector undergoes a programmed motion relative to the feed to achieve the maximum antenna gain at every elevation angle. However, this motion introduces a time-varying phase delay to the received signal that is undesirable for wideband VLBI.

During wideband VLBI data acquisition at the 70-m antennas, the subreflector motion is usually disabled and the subreflector placed in a position that gives the best gain for a 45° elevation angle. This eliminates the time-varying phase delay associated with subreflector motion. However, it also causes some loss of antenna gain when the antenna is not at 45°.

Subreflector motion should not be disabled when a BWG antenna is used for wideband VLBI observations in the Ka-band. This is because gravity deformation also affects antenna pointing by an amount that is significant at Ka-band although not so at S- or X-bands and subreflector motion must be enabled in order to have the antenna point as commanded. The resultant phase delay changes can be modeled and removed in post processing.

2.3.3 *Data Acquisition*

The analog IF signals from each antenna are routed to an IF Gain Control (IFG) assembly and then digitized by the IF Digitizer (IFD). The IFD channelizes the IF band and sends digital packets through the Digital IF Switch (DIS) to the VRA. The VRA converts digital packets into digital baseband channels which are recorded to disk. The VRA can output up to 16 baseband channels. The VRA can record digital channels as either complex in-phase and quadrature (IQ) samples or real upper sideband and lower sideband (USB/LSB) samples.

The outputs of the baseband channel are placed into recording frames along with timing and parity data, and sent to the EJVC via internet. Supported channel bandwidths vary from 200 Hz to 100 MHz as shown in Table 2. Allowed channel bandwidths are enumerated by

combining the multiplier in the top row and the first column, with units for each row in the right column. The x1 channel bandwidth column is shaded gray to indicate that these values are redundant with the final column.

Table 2. Supported Bandwidths

Multiplier	X 1	X 1.25	X 1.6	X 2	X 2.5	X 3.2	X 4	X 5	X 6.4	X 8	X 10	Unit
10 MHz	10	12.5	16	20	25	32	40	50	64	80	100	MHz
1 MHz	1	1.25	1.6	2	2.5	3.2	4	5	6.4	8	10	MHz
100 kHz	100	125	160	200	250	320	400	500	640	800	1000	kHz
10 kHz	10	12.5	16	20	25	32	40	50	64	80	100	kHz
1 kHz	1	1.25	1.6	2	2.5	3.2	4	5	6.4	8	10	kHz
100 Hz	--	--	--	200	250	320	400	500	640	800	1000	Hz

The maximum supported data rate is currently 2.048 Gbit/sec. For example, 16 complex channels with 32 MHz bandwidth and 2-bit sample resolution could be recorded. Bit configurations of 4 and 8 are also supported, as long as the maximum supported bitrate is not exceeded. For example, 4 complex channels with 8 bits is supported for channel bandwidth up to 32 MHz.

2.3.4 *Phase Calibration Tones*

The 70-m antennas include "S-band and X-band" tone generators (Reference 4). The tone generators inject a set of tones, uniformly spaced in frequency, into the receive signal path ahead of the LNA. The purpose of these tones is to permit calibration of irregularities in phase delay occurring along the signal path to the VRA. The tones are spaced 1.0 MHz apart and are derived from the station frequency reference. The power in the phase calibration tones is less than 1% of the signal power in any given bandwidth. With such a small power, the phase calibration tones do not interfere with the VLBI measurements. The 1.0 MHz spacing guarantees that at least one tone will be present in each 2-MHz or greater bandwidth normally used for VLBI. Selection of channel center frequencies will assure that one tone will be present in one sideband of each channel for narrower bandwidths.

The 34-m BWG antennas, DSS-25, -35, -53, and -55 have X/Ka (X-band and Ka-band) tone generators. The other BWG antennas, DSS-26, -34, -54, and -56 have both S/X (S-band and X-band) and X/Ka tone generators. The X/Ka tone generators have a tone spacing of 4.0 MHz. The tones are derived from the station frequency reference.

There is no simultaneous S/X and X/Ka-band tones available at any antennas. DSS tone generator availability is shown in Table 3.

Table 3. Tone Generator Availability

DSS	Tone Generator Availability	
	S/X	X/Ka
14	✓	
24**		
25		✓
26	✓*	✓
34	✓	✓*
35		✓
36	✓	
43	✓	
53		✓
54	✓*	✓
55		✓
56	✓*	✓
63	✓	

Note: * Preselected (default) configuration
          ** It does not have a tone generator

In the VLBI correlator, a measurement is made of the relative phase delay of the calibration tone in each channel. This is accomplished by correlating the recorded channel with a local (baseband) model of the individual calibration tone. These phase delay measurements enable the phase slope of the entire instrumentation system to be estimated and any phase offsets introduced across the analog RF and IF input to be removed. The result is a group delay calibration with a precision of 0.0015 ns for a 100-s integration time.

In addition to the precise measurement of phase delay in post processing at the VLBI correlator, the phase calibration tones are also monitored in near real-time by the VRA to detect instrument and configuration problems.

2.3.5 Correlation

The EJVC accepts VLBI data in Raw Data Exchange Format (RDEF) as specified in DSN external interface document 820-13, 0222-Science. The recorded data from two antennas may be cross-correlated. When the recorded data from one antenna are cross-correlated with that of another antenna, an interferometer is formed and the differential delay for that interferometer is determined. These correlated VLBI data are used for several purposes including navigation support, and reference frame support.

2.4 Experiment Design

The configuration and sequence of events for any wideband VLBI experiment are defined in a VLBI experiment (VEX) file as specified in DSN external interface document 820-

013, 0200-Science-VLBI. The VEX file is a format invented by members of the VLBI community to prescribe a complete description of a VLBI experiment, including scheduling, data-taking and correlation. For more information regarding these interface specifications users may contact their DSN Mission Interface Manager. Parameters from the VEX file are read by the EJVC, and the EJVC generates a recording script for the VRA and a .nmc file for antenna controller. The VRA creates an experiment log file and controls data recording.

The two observation bands (S, X, K, or Ka) for the experiment are chosen subject to the band availability on the antenna being used. A set of channels is defined for each observation band. In order to achieve high precision, the span of channel frequencies (within the band) should be wide. The two outermost channels determine this precision. The other channels are needed to resolve the phase ambiguity. Simultaneous measurements at "S- and X-band" or "X- and Ka-band" enable the differential delay in the ray path to the two observing stations caused by the Earth's ionosphere to be calibrated (Reference 1).

Baseband channels can be recorded as complex samples or as real samples from the corresponding pair of upper and lower sidebands. A lower sideband/upper sideband (LSB/USB) channel pair is created from an individual complex (I/Q) channel. At each complex, 16 complex channels may be used simultaneously resulting in a maximum of 32 real channels. Each of the 16 complex channels can be placed independently in either of the observational bands. A typical set of channel-pair frequencies is shown in Table 4 and Table 5 for simultaneous observation in the S- and X-bands or X- and Ka-bands. Also shown in Table 4 and 5 is the IF center frequency for complex channel that corresponds to the channel pair frequency. It may be noticed that the channel pair frequency equals the IF center frequency plus that of the first downconverter (2.0 GHz for S-band, 8.1 GHz for X-band, and 31.7 GHz for Ka-band).

Each channel is digitized with a selected depth of 2 bits per sample resolution. The sampling rate is at the nominal Nyquist rate (2 samples per period). The resultant parallel digital streams are formatted, time-tagged and recorded in the RDEF. The RDEF data can be translated to VLBI Data Interchange Format (VDIF), as specified in DSN external interface document 820-013 0200-Science-VLBI, for non-DSN correlators.

Table 4. Typical Channels (S- and X-Bands) for Wideband VLBI

Channel Pair	IF Center Frequency
2204.49 MHz LSB & USB	204.49 MHz
2212.49 MHz LSB & USB	212.49 MHz
2239.49 MHz LSB & USB	239.49 MHz
2259.51 MHz LSB & USB	259.51 MHz
2295.51 MHz LSB & USB	295.51 MHz
8214.49 MHz LSB & USB	114.49 MHz
8222.49 MHz LSB & USB	122.49 MHz
8238.49 MHz LSB & USB	138.49 MHz
8270.49 MHz LSB & USB	170.49 MHz
8353.51 MHz LSB & USB	253.51 MHz
8424.51 MHz LSB & USB	324.51 MHz
8520.51 MHz LSB & USB	420.51 MHz
8567.51 MHz LSB & USB	467.51 MHz
8575.51 MHz LSB & USB	475.51 MHz

Table 5. Typical Channels (X- and Ka-Bands) for Wideband VLBI

Channel Pair	IF Center Frequency
8218.01 MHz LSB & USB	118.01 MHz
8262.01 MHz LSB & USB	162.01 MHz
8346.01 MHz LSB & USB	246.01 MHz
8514.01 MHz LSB & USB	414.01 MHz
8598.01 MHz LSB & USB	498.01 MHz
31818.01 MHz LSB & USB	118.01 MHz
31850.01 MHz LSB & USB	150.01 MHz
31882.01 MHz LSB & USB	182.01 MHz
31914.01 MHz LSB & USB	214.01 MHz
31942.01 MHz LSB & USB	242.01 MHz
32014.01 MHz LSB & USB	314.01 MHz
32158.01 MHz LSB & USB	458.01 MHz
32190.01 MHz LSB & USB	490.01 MHz
32222.01 MHz LSB & USB	522.01 MHz
32254.01 MHz LSB & USB	554.01 MHz
32286.01 MHz LSB & USB	586.01 MHz

Appendix A
References

1. O. J. Sovers, J. L. Fanselow, and C. S. Jacobs, "Astrometry and Geodesy with Radio Inteferometry: Experiments, Models, Results," *Reviews of Modern Physics, Vol. 70, No. 4,* The American Physical Society, October, 1998

2. A. E. E. Rogers, "Very long baseline interferometry with large effective bandwidth for phase-delay measurements," *Radio Science Volume 5, Number 10, pp. 1239–1247*, October 1970.

3. A. R. Whitney, "Mark 5 Disk-Based Gbps VLBI Data System," in *New Technologies in VLBI*, edited by Y. C. Minh, ASP Conference Series, Vol. 306, Astronomical Society of the Pacific, San Francisco, CA, 2003.

4. R. Hamell, B. Tucker, M. Calhoun, "Phase Calibration Generator," *IPN Progress Report 42-154*, Jet Propulsion Laboratory, Pasadena, CA, October 15, 2003.